Journal of chemical & engineering data

Article

Cite This: J. Chem. Eng. Data XXXX, XXX, XXX−XXX

pubs.acs.org/jced

# Densities and Phase Equilibria of Hydrogen, Propane, and Vegetable Oil Mixtures: Experimental Data and Thermodynamic Modeling

Pablo E. Hegel,[†] Natalia S. Cotabarren,[†] Esteban A. Brignole,[†] and Selva Pereda*[,†,‡]

[†]Planta Piloto de Ingeniería Química (PLAPIQUI), Chemical Engineering Department, Universidad Nacional del Sur (UNS) - CONICET, Camino La Carrindanga Km7, 8000B Bahía Blanca, Argentina

[‡]Thermodynamics Research Unit, Chemical Engineering Department, School of Engineering, University of KwaZulu-Natal, Howard College Campus, King George V Avenue, Durban 4041, South Africa

**ABSTRACT:** Heterogeneous catalytic gas−liquid reactions are intensified when carried out in the homogeneous fluid phase by means of a supercritical cosolvent. For instance, supercritical propane is used to enhance the yield in hydrogenation of vegetable oils. Besides phase equilibrium knowledge, volumetric information is also needed to elucidate kinetic mechanisms and design continuous supercritical reactors. In this work, we report new experimental *PvT* data on the reactive mixture $H_2$ + sunflower oil + propane using the isochoric method. In addition, the phase equilibria and *PvT* data are modeled with the GCA and RK−PR equations of state, respectively. The isochoric method provides not only *PvT* information under the reaction conditions but also the reactive system compressibility, which is a key variable to attain enhanced transport properties in supercritical reactors.

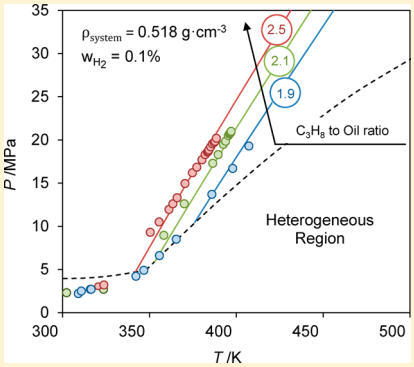


## 1. INTRODUCTION

Supercritical reactors have great potential application in heterogeneously catalyzed hydrogenation of nonvolatile substrates, taking into account the low solubility of hydrogen in condensed phases and the mass transfer limitation at the gas−liquid and liquid−solid interfaces. Several studies[1−4] have shown a great increase in the hydrogenation rate under homogeneous supercritical conditions. On the other hand, other contributions[5−8] have demonstrated that fine-tuning of the hydrogenation selectivity can also be attained. Consequently, supercritical reactors can lead to important process intensification when properly designed.

Baiker[2,9] has stressed the need to know and control the phase conditions to understand the results obtained when operating high-pressure reactors. In addition, the supercritical hydrogenation process can be carried out in batch or continuous reactors; in either case, knowledge of the volumetric properties is needed to elucidate the reaction mechanism and kinetics as well as to estimate the residence time in continuous reactors.

An interesting example of yield enhancement by operation in a supercritical medium is provided by hydrogenation of vegetable oil in supercritical propane, which shows reaction rates 3 orders of magnitude higher than that of the conventional process. Rovetto and co-workers[10,11] measured the phase equilibria of typical supercritical hydrogenation mixtures of vegetable oil, fatty esters, alcohols, and cosolvents. On the basis of these experimental data, Pereda and co-workers[12,13] upgraded the group contribution with association (GCA) equation of state (EOS)[14,15] to model these highly size-asymmetric mixtures over wide ranges of temperature and pressure. Furthermore, Pereda et al.[16] proposed a methodology to find process conditions to ensure that the hydrogenation reaction takes place in the supercritical state over the whole reaction coordinate. Following this approach, the cosolvent concentration and pressure are selected for a given operating temperature.

In general, equations of state that can describe the complex phase behavior of highly asymmetric systems fail to correlate and predict accurately the mixture volumetric properties. In this regard, Cismondi and Mollerup[17] showed the limitation of the classic cubic equations of state to predict *PvT* properties and proposed a three-parameter equation, namely, the Redlich−Kwong−Peng−Robinson (RK−PR) EOS, which was applied successfully to highly asymmetric mixtures, for instance, triglycerides and esters with methanol.[18]

A literature search shows that there are scarce experimental *PvT* data of hydrogen with heavy substrates. For instance, to the best of our knowledge, there are no data available for mixtures of triglycerides, propane, and hydrogen under liquid and supercritical conditions. In this work, we measured the densities of binary and ternary mixtures of sunflower oil, propane, and hydrogen using an isochoric apparatus[19−21] under conditions typical of vegetable oil supercritical hydrogenation. In addition, density data for the liquid phase were also measured. Finally, we modeled the new experimental data with

**Special Issue:** In Honor of Cor Peters

**Received:** September 1, 2017
**Accepted:** November 17, 2017




DOI: 10.1021/acs.jced.7b00784
J. Chem. Eng. Data XXXX, XXX, XXX−XXX

the RK−PR EOS in the homogeneous regions predicted by the GCA EOS.

## 2. MATERIALS AND METHODS

The chemicals used in the present study were hydrogen (99.99 wt %) and propane (99.9 wt %), purchased from Air Liquide and Indura SA (both from Buenos Aires, Argentina), respectively, and high-oleic sunflower oil (Dow Agrosciences, Bahía Blanca, Argentina). Analytical grade hydrogen and propane were used as received without further purification. On the other hand, in order to eliminate dissolved air and humidity, the sunflower oil was subjected to vacuum at 313 K for 24 h prior to the experimental measurements. The fatty acid profile of the latter, according to gas chromatography (GC) analysis (BS EN 14105:2003), showed about 87% oleic acid (C18:1), 7% palmitic acid (C16:0) and 6% linoleic acid (C18:2).

The isochoric apparatus used for the *PvT* measurements operates according to a synthetic method. The experimental setup and measuring procedure have been explained extensively elsewhere.[19−21] In this work, the *PvT* measurements were carried out in an isochoric high-pressure cell with a volume of ca. 12.5−13.0 $cm^3$ (Figure 1). Briefly, it consists of a high-pressure stainless steel tube (10.5 mm inside diameter) with Swagelok adapters to connect a Matheson pressure gauge (±1.5% of full scale; 25 MPa), a type-K thermocouple with a 304L stainless steel sheath (±0.1 K), and an on−off high-pressure/temperature valve with Teflon gasket seals. The cell is assembled in a solid bath made of an aluminum block with 300 W electric heating cartridges placed inside an isolated box; the temperature is controlled by an electronic thermostat (Novus N321).

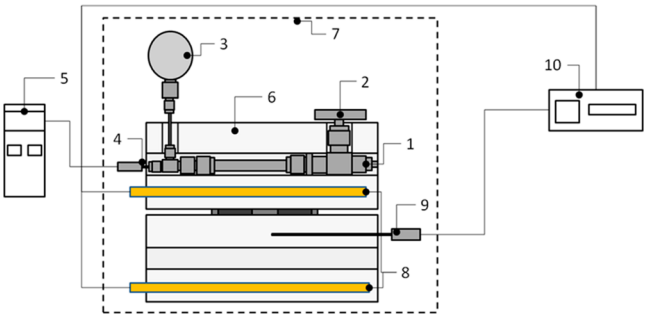


**Figure 1.** Schematic diagram of the high-pressure isochoric apparatus: (1) isochoric high pressure cell; (2) feeding valve; (3) pressure sensor; (4, 5) cell temperature sensor and indicator, respectively; (6) solid aluminum block; (7) isolated metal box (8) heating cartridges; (9, 10) temperature sensor and controller of the solid bath system, respectively.

The volume of the cell and coupled lines was first measured approximately by liquid displacement. In order to improve the accuracy of this key variable, we measured the saturation conditions for different known amounts of propane fed to the cell. With the saturation pressure and temperature, the density of the system is available in the National Institute of Standards and Technology (NIST) database,[22] from which the volume of the system can be inferred. The average of four measurements indicated that the volume of the system was 12.76 ± 0.09 $cm^3$. On the other hand, the pressure gauge was calibrated with a dead-weight tester (Fluke model 3224) and the temperature sensor with a dry-block temperature calibrator (Isotech, Fast-cal series). The whole apparatus was calibrated using pure propane as a reference fluid, and the measurements were compared to *PvT* data from NIST. Figure 2 compares the experimental

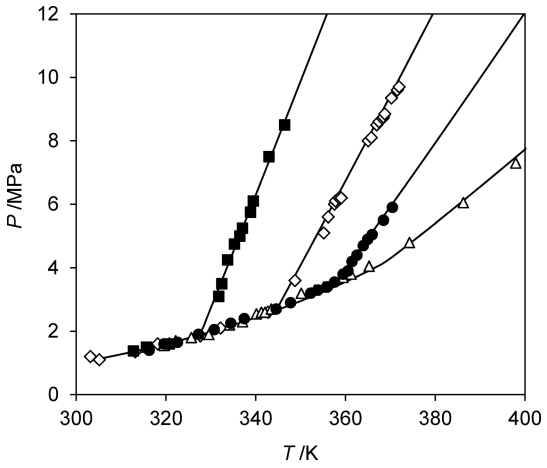


**Figure 2.** *PvT* data for pure propane at constant density. Symbols represent experimental data measured in this work: ■, 0.44 g·$cm^{-3}$; ◇, 0.40 g·$cm^{-3}$; ●, 0.36 g·$cm^{-3}$; △, 0.28 g·$cm^{-3}$. Lines show experimental data from NIST.

pressure−temperature measurements at four constant densities of pure propane with the corresponding values from the NIST database. In the homogeneous region, experiments yielded the typical isochoric pressure−temperature straight lines. The intersections of the isochoric lines with the propane vapor pressure curve correspond to the saturated liquid densities. The good agreement with the NIST data indicated that the temperature and pressure sensors were well-calibrated, as was the volume of the cell.

Initially, the high-pressure cell was purged with hydrogen and subjected to high vacuum (Welch DuoSeal 1402 vacuum pump) to eliminate the air and any gas content inside the system. Later, hydrogen was loaded into the cell (between ca. 5 and 16 mg). In order to control the loading of this compound, a gas-dosing device was built in our workshop and calibrated to determine gravimetrically the amount of gas charged to the system. Basically, this auxiliary device was first charged and weighed in an analytical balance (Sartorius Entris 224-1S, ± 0.0001 g). Then it was connected to the feed of the cell and allowed to equilibrate with the system. Finally, the gas-dosing device was weighed again to determine the mass fed into the cell and the density of the system under the loading conditions. The uncertainty in the mass of hydrogen was ±0.2 mg according to different tests carried out in the laboratory. Second, propane was injected to the system using a high-pressure syringe (also built in our workshop) that was previously calibrated to measure the mass load of solvent. Finally, the vegetable oil was fed using a manual pressure generator (HiP model 62-6-10) that was initially pressurized up to 15 MPa to avoid back flow of the gas to the oil reservoir during the loading procedure. The precise amounts of propane (between ca. 2 and 5 g) and vegetable oil (between ca. 2 and 7 g) loaded into the equipment were determined using a precision balance (Sartorius Entris 5201-1S, ±0.1 g) by directly weighing the high-pressure cell after charging with each compound. Error propagation analysis indicated that the uncertainty in the density values was about 1.5% based on


DOI: 10.1021/acs.jced.7b00784
J. Chem. Eng. Data XXXX, XXX, XXX−XXX

the accuracy of the masses of each component loaded into the cell.

The *PvT* measurements using the isochoric method consisted of loading a given amount of mixture of known composition and recording pressure−temperature pairs at a constant density. The first runs were prospective experiments, setting a fast heating of the system in order to evaluate the pressure−temperature trajectories in the liquid−vapor and single-liquid or supercritical phase regions. Finally, *PvT* measurements were carried out by increasing the temperature in steps of 10 K and recording the pressure after stable conditions were reached (approximately 30 min). As an example, Figure 3 shows a typical pressure−temperature trajectory, in which two regions of linear behavior can be seen. In addition, the sudden change in the slope (i.e., in the system compressibility) is an indication of a saturation point, where the vapor phase collapses.

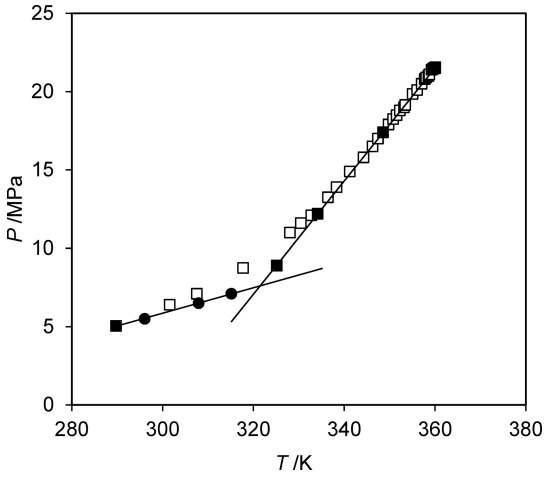


**Figure 3.** Typical pressure−temperature trajectory of the ternary system propane (1) + vegetable oil (2) + hydrogen (3) with $x_1$ = 91.9%, $x_2$ = 3.9%, and $x_3$ = 4.1% at a constant density of 0.603 g·cm$^{-3}$. Symbols represent experimental data: □, high heating rate; ●, liquid−vapor equilibria stable points; ■, single dense phase stable points. Solid lines are linear interpolations to help visualization.

In order to discard thermal degradation, the oil samples used in the experimental measurements were analyzed by GC according to protocols reported in previous works.[23] The analyses showed neither the presence of free fatty acids (a sign of thermal degradation) nor significant modifications in the fatty acid profile of the samples.

## 3. THERMODYNAMIC MODELING

As already introduced, homogeneous operation of supercritical reactors greatly increases the rate of vegetable oil hydrogenation reactions.[3,16] In order to set the boundaries of the homogeneous operating region, we accurately modeled the phase equilibrium of this system using the GCA EOS. Details about this model can be found elsewhere.[12,13] In this follow-up study, we aim to develop a tool to predict the *PvT* behavior in the homogeneous region. We selected the RK−PR EOS because of its simplicity and proven accuracy to represent volumetric properties.[24] The three-parameter cubic equation of state[17] is as follows:

$$P = \frac{RT}{v - b} - \frac{a}{(v + \delta_1 b)\left(v + \frac{1 - \delta_1}{1 + \delta_1} b\right)} \tag{1}$$

in which

$$a = a_c \left(\frac{3}{2 + T/T_c}\right)^k \tag{2}$$

where $P$ is the pressure, $R$ is the universal gas constant, $T$ is the temperature, $v$ is the molar volume, $b$ is the repulsive parameter, $a$ is the attractive parameter, $\delta_1$ is the third parameter in the RK−PR, $a_c$ is the critical attractive parameter for the pure compound, $T_c$ is the critical temperature of the pure compound, and $k$ is a pure-compound parameter that influences the temperature dependence of the attractive parameter.

In the RK−PR equation, the fitted $Z_c$ is related to $\delta_1$ by the following equation:

$$Z_c = \frac{y}{3y + d_1 - 1} \tag{3}$$

where $y$ and $d_1$ are intermediate variables:

$$d_1 = \frac{1 + \delta_1^2}{1 + \delta_1} \tag{4}$$

$$y = 1 + [2(1 + \delta_1)]^{1/3} + \left(\frac{4}{1 + \delta_1}\right)^{1/3} \tag{5}$$

The repulsive parameter and the critical value of the attractive parameter are calculated as follows:

$$b = \Omega_b \frac{RT_c}{P_c} \tag{6}$$

$$a_c = \Omega_a \frac{(RT_c)^2}{P_c} \tag{7}$$

where $\Omega_a$ and $\Omega_b$ are functions of the third parameter:

$$\Omega_a = \frac{3y^2 + 3yd_1 + d_1^2 + d_1 - 1}{(3y + d_1 - 1)^2} \tag{8}$$

$$\Omega_b = \frac{1}{3y + d_1 - 1} \tag{9}$$

Finally, we applied the RK−PR EOS using the mixing rules originally proposed by van der Waals:[25]

$$a = \sum_{i=1}^{N} \sum_{j=1}^{N} x_i x_j a_{ij} \tag{10}$$

$$a_{ij} = \sqrt{a_i a_j} \tag{11}$$

$$b = \sum_{i=1}^{N} \sum_{j=1}^{N} x_i x_j b_{ij} \tag{12}$$

$$b_{ij} = \frac{b_i + b_j}{2} \tag{13}$$

where $N$ is the number of components in the multicomponent mixture, $i$ and $j$ are the components of the mixture, and $x_i$ and $x_j$ are the mole fractions of components $i$ and $j$, respectively. On


DOI: 10.1021/acs.jced.7b00784
J. Chem. Eng. Data XXXX, XXX, XXX−XXX

the other hand, a linear mixing rule is set for the third parameter: $\delta_1 = \sum_{i=1}^{N} x_i\delta_i$.

It is important to highlight that the RK−PR EOS was used only to predict *PvT* data in the homogeneous region. Moreover, the predictions are based on pure-component parameters, i.e., without fitting of binary interaction parameters.

## 4. RESULTS AND DISCUSSION

The hydrogenation reaction is typically carried out at temperatures between 373 and 423 K,[16] a range that sets the window of the needed density data. Table 1 reports the experimental conditions and compositions for each isochoric study performed in this work. Specifically, the table includes the loaded global density, the reactant molar ratio ($H_2$ to vegetable oil), and the solvent (propane) content on a mass basis. In addition, we included the composition of the mixture on a molar basis. We first measured binary mixtures, free of hydrogen, followed by the ternary mixtures. The binary mixture runs consisted of high-density experiments; therefore, the homogeneous *PvT* data correspond to the liquid-phase region. In the case of the ternary mixtures, smaller masses were loaded into the cell in order to reach a temperature around 400 K at pressures below 25 MPa along the isochoric trajectories.

**Table 1. Experimental Conditions for Each Isochoric Experiment for the System Propane (1) + Sunflower Oil (2) + Hydrogen (3)[a]**

| Run | $\rho$/(g·cm$^{-3}$) | $H_2$ to oil molar ratio | $w_1$/(% g·g$^{-1}$) | Composition (molar basis) $x_1$ | $x_2$ | $x_3$ |
|---|---|---|---|---|---|---|
| | | | Binary Mixtures | | | |
| 1 | 0.737 | – | 35.1 | 0.916 | 0.084 | – |
| 2 | 0.658 | – | 40.5 | 0.932 | 0.068 | – |
| 3 | 0.682 | – | 30.0 | 0.896 | 0.104 | – |
| | | | Ternary Mixtures | | | |
| 4 | 0.518 | 1.2 | 71.2 | 0.958 | 0.019 | 0.0224 |
| 5 | 0.518 | 1.1 | 65.1 | 0.948 | 0.025 | 0.0267 |
| 6 | 0.518 | 1.2 | 68.1 | 0.952 | 0.022 | 0.0256 |
| 7 | 0.534 | 2.0 | 70.5 | 0.942 | 0.020 | 0.0390 |
| 8 | 0.572 | 0.5 | 54.8 | 0.942 | 0.039 | 0.0192 |
| 9 | 0.573 | 1.2 | 61.6 | 0.937 | 0.029 | 0.0340 |
| 10 | 0.541 | 0.9 | 59.4 | 0.941 | 0.032 | 0.0273 |
| 11 | 0.502 | 1.0 | 68.7 | 0.957 | 0.022 | 0.0215 |
| 12 | 0.636 | 1.3 | 40.7 | 0.858 | 0.062 | 0.0800 |
| 13 | 0.557 | 1.7 | 53.4 | 0.897 | 0.039 | 0.0640 |
| 14 | 0.565 | 1.7 | 59.6 | 0.918 | 0.031 | 0.0510 |

[a]The standard uncertainties $u$ are $u(x_1) = 0.002$, $u(x_2) = 0.001$, and $u(x_3) = 0.001$.

Runs 4 to 6 in Table 1 depict the system behavior when the global density is constant for three similar mixtures. These three runs allow an evaluation of the sensitivity of the *PvT* data to small changes in composition. On the other hand, runs 7 and 8 compare different hydrogen to oil molar ratios (2 and 0.5) for an apparent constant propane composition (94.2% on a molar basis). However, because of the high asymmetry in molecular weight of the system components, the mixture with a lower oil content also has a higher propane concentration on a weight basis (70.5% vs 54.8%), which is a significant difference.

Tables 2 and 3 report the pressure ($P$)−temperature ($T$) trajectories (isochoric lines) for the binary and ternary systems, respectively. The reader can find more discussion about the experimental results in the last section, along with the modeling work.

**Table 2. Isochores for the Propane (1) + Sunflower Oil (2) Binary System[a,b]**

| $T$/K | $P$/MPa | $T$/K | $P$/MPa | $T$/K | $P$/MPa |
|---|---|---|---|---|---|
| Run 1 | | Run 2 | | Run 3 | |
| $\rho$ = 0.737 g·cm$^{-3}$ | | $\rho$ = 0.658 g·cm$^{-3}$ | | $\rho$ = 0.682 g·cm$^{-3}$ | |
| (0.916, 0.084) | | (0.932, 0.068) | | (0.896, 0.104) | |
| 294.8 | 2.7 | 359.6 | 5.1 | 400.1 | 8.2 |
| 297.4 | 5.7 | 364.0 | 7.7 | 410.5 | 11.2 |
| 299.8 | 7.7 | 368.0 | 9.2 | 421.8 | 15.7 |
| 302.7 | 9.7 | 378.5 | 14.2 | 432.5 | 19.7 |
| 305.1 | 11.7 | 388.8 | 18.9 | | |
| 308.0 | 13.7 | | | | |
| 311.0 | 15.7 | | | | |
| 313.6 | 17.7 | | | | |
| 316.0 | 19.2 | | | | |
| 318.3 | 20.7 | | | | |

[a]The standard uncertainties $u$ are $u(\rho) = 0.009$ g·cm$^{-3}$, $u(T) = 0.1$ K, and $u(P) = 0.37$ MPa. [b]The density $\rho$ and the molar composition ($x_1$, $x_2$) are given for each run.

**4.1. Pure-Component Thermodynamic Modeling.** The nature of the three components under study is so dissimilar that a different approach is needed to model each of them. Under the typical reactor operating conditions (373 to 423 K and up to 30 MPa), hydrogen is a permanent gas, propane is a condensable gas (near its critical region), and the vegetable oil is a nonvolatile heavy substrate with almost no vapor pressure. Table 4 gives the properties available for each pure component.

In the case of hydrogen and propane, we followed the approach suggested by Cismondi and Mollerup,[17] who set $Z_c^{EOS} = 1.168 \cdot Z_c^{exp}$ to calculate the parameter $\delta_1$ of the RK−PR EOS. Next, the parameters $a_c$, $b$, and $k$ were fitted to the pure-component critical properties and acentric factor. Table 5 reports the parameters calculated for both gases, and Figure 4 shows the accuracy of the RK−PR EOS in correlating their high-pressure, high-temperature *PvT* data.[22] The RK−PR EOS is able to correlate the hydrogen and propane data shown in Figure 4 with deviations in pressure of 1.9% and 7.4%, respectively.

Since critical and vapor−liquid equilibrium properties of vegetable oils are not available, a different approach was needed to set their pure-component parameters. The critical properties reported in Table 4 are linear extrapolations of the data measured by Bogatishcheva et al.[27] for low- to medium-weight triglycerides. On the other hand, we set the other pure-component parameters by fitting density[28] and solubility parameter ($\delta$)[29] data, taking into account that the latter are directly related to the molar density as follows:[30] $\delta = \alpha^{1/2} \cdot \rho$. Figure 5 depicts the accurate RK−PR EOS correlations of the available experimental density and solubility parameter data (average relative deviation (ARD) = 2.02% and 1.63%, respectively).

As mentioned above, we predicted the boundaries of the homogeneous region with the GCA EOS. This is a group contribution model that allows prediction of the phase behaviors of different oils by just changing the groups that make up the heavy molecule. In this work, we used the binary interaction parameters reported by Pereda et al.,[13] who fitted the ternary mixture $H_2$ + propane + tripalmitin. However, we


DOI: 10.1021/acs.jced.7b00784
J. Chem. Eng. Data XXXX, XXX, XXX−XXX

Table 3. Isochores for the Propane (1) + Sunflower Oil (2) + Hydrogen (3) Ternary System[a,b]

| T/K | P/MPa | T/K | P/MPa | T/K | P/MPa | T/K | P/MPa |
|---|---|---|---|---|---|---|---|
| Run 4: $\rho$ = 0.518 g·cm$^{-3}$ (0.958, 0.019, 0.022) | | Run 6: $\rho$ = 0.518 g·cm$^{-3}$ (0.952, 0.022, 0.026) | | Run 9: $\rho$ = 0.573 g·cm$^{-3}$ (0.937, 0.029, 0.034) | | Run 12: $\rho$ = 0.636 g·cm$^{-3}$ (0.858, 0.062, 0.08) | |
| 350.5 | 9.3 | 358.3 | 9.0 | 334.5 | 8.7 | 359.8 | 15.2 |
| 355.6 | 10.5 | 370.1 | 12.6 | 339.0 | 9.7 | 364.3 | 16.7 |
| 361.3 | 12.0 | 386.5 | 17.3 | 349.3 | 13.7 | 367.8 | 17.8 |
| 363.5 | 12.6 | 389.6 | 18.3 | 355.6 | 16.0 | 370.5 | 18.7 |
| 366.0 | 13.3 | 392.6 | 19.5 | 367.1 | 20.7 | 385.5 | 24.6 |
| 370.5 | 15.0 | 393.9 | 19.9 | 373.5 | 23.3 | | |
| 374.8 | 16.2 | 395.5 | 20.5 | | | Run 13: $\rho$ = 0.557 g·cm$^{-3}$ (0.897, 0.039, 0.064) | |
| 377.3 | 16.9 | 396.1 | 20.7 | Run 10: $\rho$ = 0.541 g·cm$^{-3}$ (0.941, 0.032, 0.027) | | | |
| 380.3 | 17.7 | 396.6 | 20.8 | | | 362.0 | 10.8 |
| 382.1 | 18.3 | 396.7 | 20.8 | 357.3 | 6.1 | 374.8 | 13.5 |
| 383.5 | 18.6 | 397.0 | 20.9 | 366.3 | 7.7 | 392.0 | 17.7 |
| 384.0 | 18.7 | 397.1 | 21.0 | 366.6 | 7.8 | 396.7 | 18.5 |
| 384.3 | 18.9 | | | 376.3 | 9.3 | | |
| 385.3 | 19.2 | Run 7: $\rho$ = 0.534 g·cm$^{-3}$ (0.942, 0.02, 0.039) | | 388.0 | 11.8 | Run 14: $\rho$ = 0.565 g·cm$^{-3}$ (0.918, 0.031, 0.051) | |
| 386.3 | 19.6 | | | 411.2 | 16.2 | | |
| 387.3 | 19.7 | 342.5 | 8.0 | | | 335.3 | 11.5 |
| 387.8 | 19.9 | 351.1 | 10.2 | Run 11: $\rho$ = 0.502 g·cm$^{-3}$ (0.957, 0.022, 0.022) | | 342.3 | 14.3 |
| 388.6 | 20.2 | 360.6 | 13.0 | | | 349.3 | 17.7 |
| | | 371.3 | 15.9 | 355.6 | 6.8 | 359.8 | 20.7 |
| Run 5: $\rho$ = 0.518 g·cm$^{-3}$ (0.948, 0.025, 0.027) | | 380.3 | 18.8 | 369.3 | 10.1 | | |
| | | 385.8 | 20.7 | 393.8 | 16.1 | | |
| 346.8 | 4.9 | | | 396.2 | 16.7 | | |
| 355.8 | 6.6 | Run 8: $\rho$ = 0.572 g·cm$^{-3}$ (0.942, 0.039, 0.019) | | 401.3 | 18.0 | | |
| 365.5 | 8.5 | | | 404.3 | 18.6 | | |
| 386.0 | 13.7 | 364.0 | 9.0 | 406.4 | 19.0 | | |
| 398.0 | 16.7 | 374.0 | 11.0 | 407.6 | 19.2 | | |
| 407.3 | 19.3 | 384.3 | 13.3 | 408.5 | 19.3 | | |
| | | 398.8 | 17.2 | 408.5 | 19.2 | | |
| | | 404.3 | 19.2 | 408.6 | 19.3 | | |

[a]The standard uncertainties $u$ are $u(\rho)$ = 0.009 g·cm$^{-3}$, $u(T)$ = 0.1 K, and $u(P)$ = 0.37 MPa. [b]The density $\rho$ and the molar composition ($x_1$, $x_2$, $x_3$) are given for each run.

Table 4. Pure-Component Properties

| Compound | MW/(g·mol$^{-1}$) | $T_c$/K | $P_c$/MPa | $v_c$/(cm$^3$·mol$^{-1}$) | $\omega$ | ref |
|---|---|---|---|---|---|---|
| Hydrogen | 2.02 | 33.2 | 1.31 | 60 | −0.216 | 26 |
| Propane | 44.1 | 369.8 | 4.25 | 200 | 0.1523 | 26 |
| Triolein[a] | 885 | 984.5 | 0.51 | – | – | 27 |

[a]Sunflower oil was modeled as triolein since oleic acid is its major fatty acid.

Table 5. RK−PR EOS Pure-Component Parameters

| Compound | $a_c$/(MPa·m$^6$·kmol$^{-2}$) | $b$/(cm$^3$·mol$^{-1}$) | $\delta_1$ | $k$ |
|---|---|---|---|---|
| Hydrogen | 0.0245 | 18.6 | 0.483 | 0.4982 |
| Propane | 0.9782 | 60.1 | 1.6206 | 1.9592 |
| Vegetable oil | 68.089 | 971.8 | 5.5 | 5.2 |

replaced the tripalmitin pure-component parameters by those for triolein reported by Espinosa et al.[31] since oleic acid is the major fatty acid of the sunflower oil.

**4.2. Binary and Ternary *PvT* Data Prediction.** On the basis of the pure-component modeling, we compared the binary and ternary *PvT* data measured in this work with RK−PR EOS predictions. Figures 6 to 9 show GCA EOS predictions of the boundaries of the heterogeneous region (dashed lines) together with RK−PR EOS predictions (solid lines) of the new *PvT* data (symbols). In particular, Figure 6 shows the results for the three isochoric high-density binary mixture data. The open symbols show the liquid−vapor behavior, which in all cases is similar to the bubble points predicted by the GCA EOS for the three runs, since the composition of the vegetable oil in the vapor phase is practically nil. In addition, the RK−PR EOS is able to fully predict the three isochores. It is worth noting that even though the higher global density system corresponds to the isochore far to the left, the one at the right does not represent the run with lower density. In several runs, we observed that changes in the mixture composition lead to a counterintuitive transformation of the *PvT* behavior of the mixture. This highlights the importance of applying a thermodynamic model with a consistent physical background to predict the experimental data instead of just developing a mathematical correlation.

Runs 4 to 6 represent three similar experimental conditions (0.518 g·cm$^{-3}$) and mixtures, whose compositions differ from one another only by 3 wt % propane (see Table 1). In


DOI: 10.1021/acs.jced.7b00784
J. Chem. Eng. Data XXXX, XXX, XXX−XXX

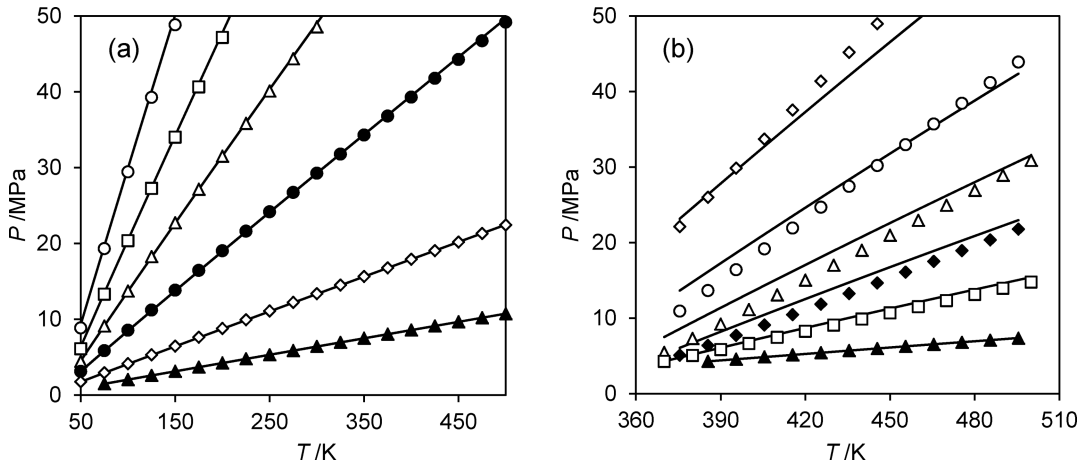


**Figure 4.** *PvT* data for supercritical compounds. (a) Hydrogen: ▲, 0.005 g·cm$^{-3}$; ◇, 0.01 g·cm$^{-3}$; ●, 0.02 g·cm$^{-3}$; △, 0.03 g·cm$^{-3}$; □, 0.04 g·cm$^{-3}$; ○, 0.05 g·cm$^{-3}$. (b) Propane: ▲, 0.1 g·cm$^{-3}$; □, 0.22 g·cm$^{-3}$; ◆, 0.3 g·cm$^{-3}$; △, 0.35 g·cm$^{-3}$; ○, 0.4 g·cm$^{-3}$; ◇, 0.45 g·cm$^{-3}$. Symbols represent experimental data,[22] and solid lines show RK−PR correlations.

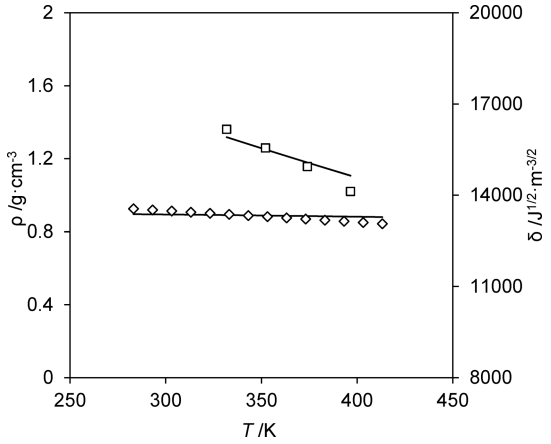


**Figure 5.** RK−PR correlations of density (◇) and solubility parameter (□) data for sunflower and soybean oil, respectively. Symbols represent experimental data,[28,29] and solid lines show RK−PR correlations.

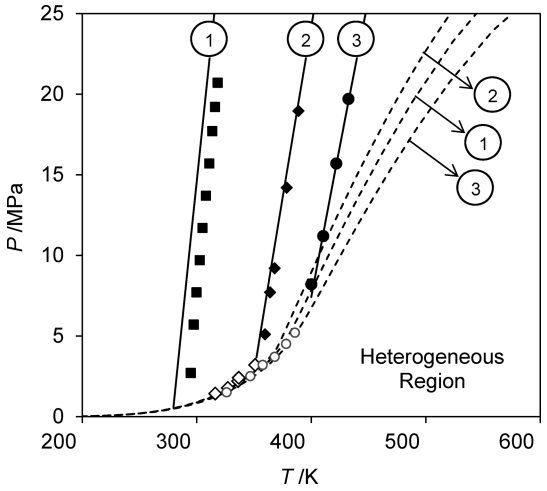


**Figure 6.** *PvT* data for the propane (1) + vegetable oil (2) binary system. Symbols represent experimental data: ■, run 1 with $\rho$ = 0.737 g·cm$^{-3}$, $w_1$ = 35.1%, $w_2$ = 64.9%; ◆ and ◇, run 2 with $\rho$ = 0.658 g·cm$^{-3}$, $w_1$ = 40.5%, $w_2$ = 59.5%; ● and ○, run 3 with $\rho$ = 0.682 g·cm$^{-3}$, $w_1$ = 30%, $w_2$ = 70%. Dashed lines show the boundaries of the heterogeneous region predicted with the GCA EOS. Solid lines show the RK−PR predictions of *PvT* data in the homogeneous region.

agreement with this, Figure 7 shows that the GCA EOS predicts almost the same phase envelope for the three mixtures. However, the isochores, which are alike in the vapor−liquid region, differ greatly in the homogeneous regions. Following this sensitivity, the RK−PR EOS is able to predict the system transformation when switching from one mixture to another.

Figure 8 compares runs 7 and 8 with different $H_2$ to oil ratios (2 and 0.5, respectively) for mixtures containing 94.2% propane (molar basis). As explained before, these two systems have a difference of almost 15 wt % in propane content (see Table 1). As can be seen, the GCA EOS predicts well the vapor−liquid equilibrium data points for each run. In addition, the RK−PR EOS qualitatively describes the stiff isochores. It is important to highlight that the model ARDs in density for the two pressure−temperature trajectories are 2.55% and 0.24%, which are good quantitative results considering that the model is fully predictive.

Finally, Figure 9 compares run 4 with run 9, which depict the same $H_2$ to oil molar ratio but different solvent content. Moreover, run 9 has lower propane and oil contents by about 10% and 1% (mass basis), respectively. The RK−PR EOS predicts both isochores in the homogeneous region with ARDs of 0.12% and 0.58%.

When it comes down to calculating the density of multicomponent mixtures involved in supercritical reactors, it is common in the literature to find studies that assume ideal solution behavior for estimating the molar volume of the reactive mixture. For an ideal solution, the molar volume of the mixture ($v^{\text{id.sol.}}$) is a linear average, weighted by the mole fractions, of the pure-compound molar volumes ($v_i$). Therefore, at the system temperature $T$, for any composition $x$ and any pressure between zero and the pressure of the mixture $P$, we obtain:

$$v^{\text{id.sol.}}(T, P, x) = \sum_{i=1}^{N} x_i v_i(T, P) \tag{14}$$

where $x_i$ is the mole fraction of component $i$ in the mixture and $N$ is the number of components. All expressions for the


DOI: 10.1021/acs.jced.7b00784
J. Chem. Eng. Data XXXX, XXX, XXX−XXX

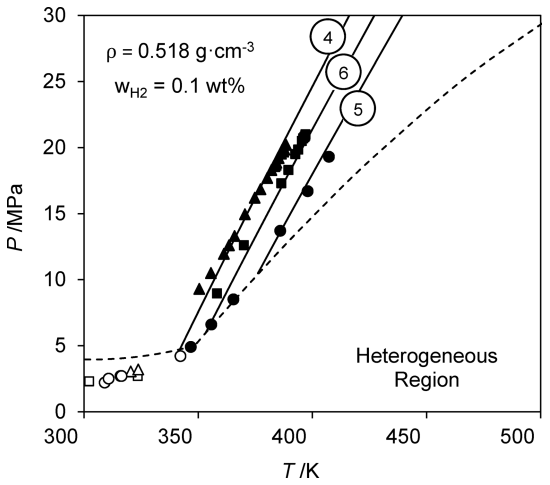


**Figure 7.** *PvT* data for propane (1) + vegetable oil (2) + hydrogen (3) at $\rho$ = 0.518 g·cm$^{-3}$ and $w_3$ = 0.1%. Symbols represent experimental data: ▲ and △, run 4 with $w_1$ = 71.2%, $w_2$ = 28.8%; ● and ○, run 5 with $w_1$ = 65.1%, $w_2$ = 34.8%; ■ and □, run 6 with $w_1$ = 68.1%, $w_2$ = 31.8%. Dashed lines show the boundaries of the heterogeneous region predicted with the GCA EOS. Solid lines show the RK−PR predictions of *PvT* data in the homogeneous region.

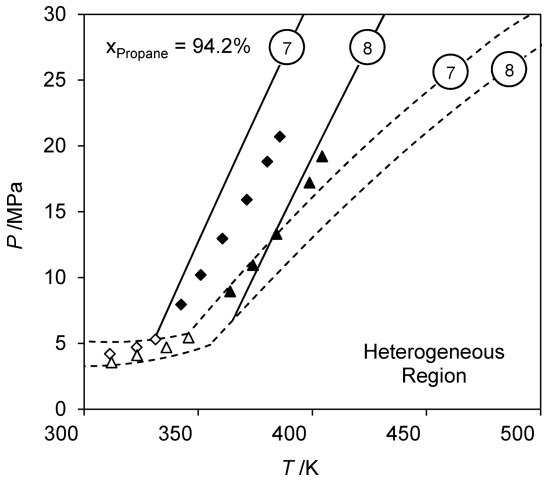


**Figure 8.** *PvT* data for the propane (1) + vegetable oil (2) + hydrogen (3) ternary system. Symbols represent experimental data: ◆ and ◇, run 7 with $\rho$ = 0.534 g·cm$^{-3}$, $w_1$ = 70.5%, $w_2$ = 29.4%, $w_3$ = 0.1%; ▲ and △, run 8 with $\rho$ = 0.572 g·cm$^{-3}$, $w_1$ = 54.8%, $w_2$ = 45.2%, $w_3$ = 0.1%. Dashed lines show boundaries of the heterogeneous region predicted with the GCA EOS. Solid lines show the RK−PR predictions of *PvT* data in the homogeneous region.

thermodynamic properties of the ideal solution can be derived from eq 14, commonly known as Amagat's law. It is important to note that, by definition, the ideal solution at fixed temperature and composition obeys Amagat's law at all pressures between zero and the pressure of the system. If Amagat's law is satisfied at a particular pressure, the system is not necessarily ideal.[25]

Zabaloy et al.[32,33] showed that classic EOSs coupled to the one-fluid approach (i.e., EOSs for which the mixture parameters are obtained as functions of composition and temperature) cannot represent ideal solutions. Therefore, the RK−PR EOS with classic mixing rules will always differ from the ideal solution, even in the case of using combination rules with no binary interaction parameters, as we are doing in this work.

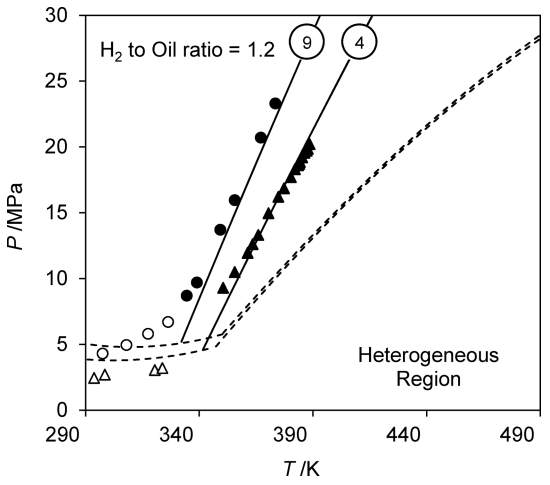


**Figure 9.** *PvT* data for propane + vegetable oil + hydrogen. Symbols represent experimental data: ● and ○, run 9 with $\rho$ = 0.573 g·cm$^{-3}$, $w_1$ = 61.6%, $w_2$ = 38.3%, $w_3$ = 0.1%; ▲ and △, run 4 with $\rho$ = 0.518 g·cm$^{-3}$, $w_1$ = 71.2%, $w_2$ = 28.8%, $w_3$ = 0.1%. Dashed lines show boundaries of the heterogeneous region predicted with the GCA EOS. Solid lines show the RK−PR predictions of *PvT* data in the homogeneous region.

Table 6 summarizes the ARDs in density for each experimental run the ideal solution assumption and the RK−PR EOS are applied in a fully predictive manner. The benefit of applying a simple cubic EOS to calculate the density is evident. It is worth mentioning that Velez et al.[23] showed the direct influence that the volumetric properties have on the residence time and reaction kinetics, both calculated rigorously and assuming ideal solutions.

Last, Table 6 also presents for each mixture the isochoric thermal pressure coefficient, $\gamma = (\partial P/\partial T)_{v,x}$, which is a measure of the system compressibility. The improvement of supercritical heterogeneously catalyzed reactions is mainly based in the possibility of controlling the reactants molar ratio (homogeneous operation) and the well-known enhanced transport properties of compressible fluids. As Table 6 shows, the value of $\gamma$ changes from 0.7444 MPa·K$^{-1}$ for the binary liquid phase (run 1) to as low as 0.1881 MPa·K$^{-1}$ (run 10). Runs 4 to 6 (very similar mixtures under the same global density) show that $\gamma$ is highly sensitive to the mixture composition. In this regard, the model developed in this work allows compressibility information to be taken into account during the phase equilibrium engineering of supercritical reactors (i.e., by setting appropriate $\gamma$ values as constraints while designing the reactive mixture that fulfills the process needs).

## 5. CONCLUSIONS

Heterogeneously catalyzed gas−liquid reactions are intensified when carried out in the homogeneous fluid phase by means of a supercritical cosolvent. Tools for predicting phase equilibria and *PvT* behavior are keys for selecting adequate solvents, designing operating windows, elucidating kinetic mechanisms, and designing continuous reactors. In this regard, hydrogenation of heavy substrates, like vegetable oils, has been highly studied because of the difficulty of sorting out mass transfer limitations and attaining fine control of the selectivity using conventional solvents. In this work, we measured new experimental *PvT* data for binary and ternary mixtures involving $H_2$, propane, and sunflower oil using the isochoric method. The


DOI: 10.1021/acs.jced.7b00784
J. Chem. Eng. Data XXXX, XXX, XXX−XXX

Table 6. Thermodynamic Modeling of Volumetric Properties: Density ($\rho$), Thermal Pressure Coefficient ($\gamma$), and Average Relative Deviations in Density (ARD($\rho$)) Assuming Ideal Solution Behavior (id.sol.) and Predicted with the RK−PR EOS

| | | | | | ARD($\rho$)/% | |
|---|---|---|---|---|---|---|
| Run | $T$/K | $P$/MPa | $\rho$/g·cm$^{-3}$ | $\gamma$/MPa·K$^{-1}$ | id.sol. | RK−PR |
| | | | Binary Mixtures | | | |
| 1 | 294.8−318.3 | 2.7−20.7 | 0.737 | 0.7444 | 4.55 | 0.81 |
| 2 | 359.6−388.8 | 5.1−18.9 | 0.658 | 0.4680 | 12.56 | 0.46 |
| 3 | 400.1−432.5 | 8.2−19.7 | 0.682 | 0.3598 | 9.77 | 0.04 |
| | | | Ternary Mixtures | | | |
| 4 | 350.5−388.6 | 9.3−20.2 | 0.518 | 0.2919 | 8.44 | 0.12 |
| 5 | 346.8−407.3 | 4.9−19.3 | 0.518 | 0.2398 | 13.85 | 1.42 |
| 6 | 358.3−397.1 | 9.0−21.0 | 0.518 | 0.3098 | 8.49 | 0.26 |
| 7 | 342.5−385.8 | 8.0−20.7 | 0.534 | 0.2931 | 13.20 | 2.55 |
| 8 | 364.0−404.3 | 9.0−19.2 | 0.572 | 0.2529 | 12.69 | 0.24 |
| 9 | 334.5−373.5 | 8.7−23.3 | 0.573 | 0.3806 | 9.19 | 0.58 |
| 10 | 357.3−411.2 | 6.1−16.2 | 0.541 | 0.1881 | 17.57 | 1.08 |
| 11 | 355.6−408.6 | 6.8−19.3 | 0.502 | 0.2370 | 10.20 | 0.18 |
| 12 | 359.8−385.5 | 15.2−24.6 | 0.636 | 0.3683 | 10.19 | 2.06 |
| 13 | 362.0−396.7 | 10.8−18.5 | 0.557 | 0.3825 | 12.96 | 2.62 |
| 14 | 335.3−359.8 | 11.5−20.7 | 0.565 | 0.2259 | 6.82 | 4.05 |

data cover the temperature range from 294.8 to 432.5 K and the pressure range from 2.7 to 24.6 MPa. In addition, we compared the data with phase envelopes predicted with the GCA EOS. Finally, we modeled the new $PvT$ data using the RK−PR EOS, which is a three-parameter cubic equation of state. On the basis of correlations of pure-component $PvT$ behavior, the RK−PR EOS accurately predicts the densities of binary and ternary mixtures in spite of the sensitivity of the data to the mixture composition and global density. It is important to highlight that using a simple equation of state, even without binary interaction parameters, is substantially more accurate that assuming ideal solution behavior.

Finally, the isochoric method provides not only $PvT$ information under the reaction conditions but also the reactive system compressibility, which is a key variable to attain enhanced transport properties.

## AUTHOR INFORMATION


### Corresponding Author

*E-mail: spereda@plapiqui.edu.ar.

### ORCID

Selva Pereda: 0000-0002-2320-4298



### Funding

The authors acknowledge the financial support granted by the Consejo Nacional de Investigaciones Científicas y Técnicas (PIP 112 2015 010 856), the Ministerio de Ciencia, Tecnología e Innovación Productiva (PICT 2016 0907 and 2014 2293), and Universidad Nacional del Sur (PGI - 24/M133).


### Notes

The authors declare no competing financial interest.

## ACKNOWLEDGMENTS


The authors are thankful to Francisco Sánchez and Marcelo Zabaloy for valuable discussions during the preparation of this article and to Professor Cor Peters for a long, fruitful cooperation.


## REFERENCES


(1) Savage, P. E.; Gopalan, S.; Mizan, T. I.; Martino, C. J.; Brock, E. E. Reactions at Supercritical Conditions: Applications and Fundamentals. *AIChE J.* **1995**, *41*, 1723−1778.

(2) Baiker, A. Supercritical Fluids in Heterogeneous Catalysis. *Chem. Rev.* **1999**, *99*, 453−474.

(3) Härröd, M.; Møller, P. Hydrogenation of Substrate and Products Manufactured according to the Process. U.S. Patent 5,962,711, 1999.

(4) Macher, M.-B. Supercritical Hydrogenation of Vegetable Oils. Doctoral Thesis, Chalmers University of Technology, Göteburg, Sweden, 2001.

(5) Wandeler, R.; Künzle, N.; Schneider, M. S.; Mallat, T.; Baiker, A. Continuous Enantioselective Hydrogenation of Ethyl Pyruvate in "Supercritical" Ethane: Relation between Phase Behavior and Catalytic Performance. *J. Catal.* **2001**, *200*, 377−388.

(6) Burk, M. J.; Feng, S.; Gross, M. F.; Tumas, W. Asymmetric Catalytic Hydrogenation Reactions in Supercritical Carbon Dioxide. *J. Am. Chem. Soc.* **1995**, *117*, 8277−8278.

(7) Bhanage, B. M.; Ikushima, Y.; Shirai, M.; Arai, M. The Selective Formation of Unsaturated Alcohols by Hydrogenation of $\alpha,\beta$-Unsaturated Aldehydes in Supercritical Carbon Dioxide Using Unpromoted Pt/$Al_2O_3$ Catalyst. Catal. *Catal. Lett.* **1999**, *62*, 175−177.

(8) Hitzler, M. G.; Smail, F. R.; Ross, S. K.; Poliakoff, M. Selective Catalytic Hydrogenation of Organic Compounds in Supercritical Fluids as a Continuous Process. *Org. Process Res. Dev.* **1998**, *2*, 137−146.

(9) Wandeler, R.; Baiker, A. In Situ Monitoring of Heterogeneously Catalyzed Reactions under Supercritical Conditions. *Chimia* **1999**, *53*, 566−569.

(10) Rovetto, L.; Bottini, S. B.; Brignole, E. A.; Peters, C. J. Supercritical Hydrogenation Processes. Experimental Results on the Fluid Phase Behavior of Binary and Ternary Mixtures of Hydrogen, Propane and Tripalmitin. *J. Supercrit. Fluids* **2003**, *25*, 165−176.

(11) Rovetto, L. J.; Peters, C. J.; Brignole, E. A. Phase Equilibrium Behavior for Hydrogenolysis Components: Three-Phase Equilibria LLV and Retrograde Behavior. *J. Supercrit. Fluids* **2005**, *34*, 183−187.

(12) Pereda, S.; Bottini, S.; Brignole, E. A. Gas-Liquid Reactions under Supercritical Conditions—Phase Equilibria and Thermodynamic Modeling. *Fluid Phase Equilib.* **2002**, *194−197*, 493−499.

(13) Pereda, S.; Rovetto, L.; Bottini, S. B.; Brignole, E. A. Phase-Equilibrium Modeling in the Hydrogenation of Vegetable Oils and Derivatives. *J. Am. Oil Chem. Soc.* **2006**, *83*, 461−467.

(14) Gros, H. P.; Bottini, S.; Brignole, E. A. A Group Contribution Equation of State for Associating Mixtures. *Fluid Phase Equilib.* **1996**, *116*, 537−544.




DOI: 10.1021/acs.jced.7b00784
J. Chem. Eng. Data XXXX, XXX, XXX−XXX

(15) González Prieto, M.; Sánchez, F. A.; Pereda, S. Thermodynamic Model for Biomass Processing in Pressure Intensified Technologies. *J. Supercrit. Fluids* **2015**, *96*, 53−67.
(16) Pereda, S.; Bottini, S. B.; Brignole, E. A. Phase Equilibrium Engineering of Supercritical Hydrogenation Reactors. *AIChE J.* **2002**, *48*, 2635−2645.
(17) Cismondi, M.; Mollerup, J. Development and Application of a Three-Parameter RK−PR Equation of State. *Fluid Phase Equilib.* **2005**, *232*, 74−89.
(18) Cotabarren, N. S.; Velez, A. R.; Hegel, P. E.; Pereda, S. Prediction of Volumetric Data in Supercritical Reactors. *J. Chem. Eng. Data* **2016**, *61*, 2669−2675.
(19) Yurttaş, L.; Holste, J. C.; Hall, K. R.; Gammon, B. E.; Marsh, K. N. Semiautomated Isochoric Apparatus for *P*−*V*−*T* and Phase Equilibrium Studies. *J. Chem. Eng. Data* **1994**, *39*, 418−423.
(20) Velez, A.; Pereda, S.; Brignole, E. A. Isochoric Lines and Determination of Phase Transitions in Supercritical Reactors. *J. Supercrit. Fluids* **2010**, *55*, 643−647.
(21) Yurttaş, L. A. New Isochoric Apparatus with Applications to *P*−*V*−*T* and Phase Equilibria Studies. Ph.D. Dissertation, Texas A&M University, College Station, TX, 1988.
(22) *NIST Chemistry WebBook*; NIST Standard Reference Database Number 69; National Institute of Standards and Technology: Gaithersburg, MD, 2005.
(23) Velez, A. R.; Soto, G.; Hegel, P. E.; Mabe, G. D. B.; Pereda, S. Continuous Production of Fatty Acid Ethyl Esters from Sunflower Oil Using Supercritical Ethanol. *Fuel* **2012**, *97*, 703−709.
(24) Martinez, S. A.; Hall, K. R. Thermodynamic Properties of Light Synthetic Natural Gas Mixtures Using the RK−PR Cubic Equation of State. *Ind. Eng. Chem. Res.* **2006**, *45*, 3684−3692.
(25) Prausnitz, J. M.; Lichtenthaler, R. N.; Gomes de Azevedo, E. *Molecular Thermodynamics of Fluid-Phase Equilibria*; Prentice Hall PTR: Upper Saddle River, NJ, 1999.
(26) *DIPPR Project 801: Evaluated Process Design Data*; American Institute of Chemical Engineers: New York, 2003.
(27) Bogatishcheva, N. S.; Faizullin, M. Z.; Popov, A. P.; Nikitin, E. D. Critical Properties, Heat Capacities, and Thermal Diffusivities of Four Saturated Triglycerides. *J. Chem. Thermodyn.* **2017**, *113*, 308−314.
(28) Esteban, B.; Riba, J. R.; Baquero, G.; Rius, A.; Puig, R. Temperature Dependence of Density and Viscosity of Vegetable Oils. *Biomass Bioenergy* **2012**, *42*, 164−171.
(29) King, J. W. Determination of the Solubility Parameter of Soybean Oil by Inverse Gas Chromatography. Leb. *und-Technologie* **1995**, *28*, 190−195.
(30) Michelsen, M. L.; Mollerup, J. M. *Thermodynamic Models: Fundamentals & Computational Aspects*, 2nd ed.; Tie-Line Publications: Holte, Denmark, 2007.
(31) Espinosa, S.; Fornari, T.; Bottini, S. B.; Brignole, E. A. Phase Equilibria in Mixtures of Fatty Oils and Derivatives with near Critical Fluids Using the GC-EOS Model. *J. Supercrit. Fluids* **2002**, *23*, 91−102.
(32) Zabaloy, M. S.; Brignole, E. A.; Vera, J. H. A Conceptually New Mixing Rule for Cubic and Non-Cubic Equations of State. *Fluid Phase Equilib.* **1999**, *158*−*160*, 245−257.
(33) Zabaloy, M. S.; Brignole, E. A.; Vera, J. H. A Flexible Mixing Rule Satisfying the Ideal-Solution Limit for Equations of State. *Ind. Eng. Chem. Res.* **2002**, *41*, 922−930.


DOI: 10.1021/acs.jced.7b00784
*J. Chem. Eng. Data* XXXX, XXX, XXX−XXX